Anal Bioanal Chem (2011) 399:1173–1180
DOI 10.1007/s00216-010-4397-x

ORIGINAL PAPER

A label-free sensing method for phosphopeptides using two-layer gold nanoparticle-based localized surface plasma resonance spectroscopy

Jen-Yi Chen · Yu-Chie Chen

Received: 14 September 2010 / Revised: 25 October 2010 / Accepted: 26 October 2010 / Published online: 8 November 2010

Abstract In this study, a new type of localized surface plasmon resonance (LSPR) sensing substrate for phosphopeptides was explored. It has been known that LSPR response for target species is larger in the near-infrared region (NIR) than in the visible region of the electromagnetic spectrum. Several types of noble metal nanoparticles (NPs) with NIR absorption capacities have been previously demonstrated as effective LSPR-sensing nanoprobes. Herein, we demonstrate a straightforward approach with improved sensitivity by simply using layer-by-layer (LBL) spherical Au NPs self-assembled on glass slides as the LSPR-sensing substrates that are responsive in the NIR region of the electromagnetic spectrum. The modified glass slide acquired an LSPR absorption band in the NIR, which resulted from the dipole–dipole interactions between Au NPs. To enable the chip to sense phosphopeptides, the surface of the glass chip was spin-coated with thin titania film (TiO_2-Glass@Au NPs). Absorption spectrophotometry was employed as a detection tool. Tryptic digest of α-casein was used as a model sample. The feasibility of using the new LSPR approach for detecting a potential risk factor leading to cancers (i.e., phosphorylated fibrinopeptide A) directly from human serum samples was demonstrated. Matrix-assisted laser desorption/ionization mass spectrometry (MALDI-MS) was used to confirm the results.

Keywords Gold nanoparticles · LSPR · Phosphopeptides · Label-free sensing

J.-Y. Chen · Y.-C. Chen (✉)
Department of Applied Chemistry,
National Chiao Tung University,
Hsinchu 300, Taiwan
e-mail: yuchie@mail.nctu.edu.tw

Introduction

One of the unique features of noble metal nanoparticles (NPs; i.e., Au NPs and Ag NPs) is their localized surface plasma resonance (LSPR) resulting from the resonance of collective excitation of the conduction electrons of NPs with incident photons. A broad band across the ultraviolet (UV) region accompanying a notable absorption band is known to appear in the visible to the near-infrared region (NIR) of the absorption spectrum [1]. The binding of specific molecules onto the surfaces of the NPs can cause a shift in the absorption band of the LSPR due to changes in the local dielectric environment on the NP surfaces [2]. Thus, an LSPR combined with a basic spectrophotometer was developed for the simple sensing method [3–6]. Specifically, absorption spectroscopy was used to investigate the changes in optical properties resulting from the biomolecular interactions on gold nanoparticles immobilized on glass substrates.

LSPR with an absorption band in the NIR region is suitable for use as a detection region given its larger red shift, as compared to the visible region when changes in the local dielectric environment on NP surfaces occurs [7–10]. Thus, optical sensors that are based on the LSPR shift in the NIR were developed. NPs with absorption bands in the NIR of electromagnetic spectrum, such as triangular Ag NPs [7], Au nanoshell [8], Au nanorods [9], and Au bipyramid [10] have been used as sensing substrate in LSPR-based optical sensors. Compared with generating different shapes of noble metal NPs, the generation of spherical Au NPs is relatively simple. Conventionally, spherical Au NPs can be easily generated by reacting $HAuCl_4$ with citrate-reducing agents [11], and thus, it should be desirable for LSPR optical sensors with a NIR absorption band to be fabricated based on spherical Au NPs alone. It has been known that

the layer-by-layer (LBL) self-assembled spherical Au NPs on glass slides (Glass@AuNPs) have an absorption band in the NIR arising from the dipole–dipole interactions between Au NPs [12–14]. Furthermore, the λ_{max} in the LSPR spectra can be simply adjusted by modifying the particle size of the spherical Au NPs.

Titania materials are known as effective adsorbents in selectively trapping phosphorylated species from complex samples [15–22]. Previously, a sensing method for phosphopeptides based on the LSPR were successfully demonstrated using titania-coated Au NPs (Au@TiO_2 NPs) as sensing substrate when immobilized on a glass slide surface [6]. A UV–Visible spectrophotometry was used as a detection tool [6]. The titania shell on the Au@TiO_2 NPs acted as the sensing substrate for phosphopeptides. Once the target species were captured by the Au@TiO_2 NPs on the glass slide, a red shift of the wavelength at the maximum absorption band in the visible region occurred due to the LSPR of the Au NPs. This is the basic principle used in the design for phosphopeptide sensing.

Herein, we alternatively use an LBL Glass@Au NPs coated with titania film (TiO_2-Glass@Au NPs), and with LSPR in the NIR region, as the sensing substrate for phosphopeptides by taking its advantages of improved sensitivity in the NIR region and ease of generation. We believed the detection limit of phosphopeptides could be further lowered to a certain level using this alternative approach. We initially used the tryptic digest of α-casein as a model to demonstrate the feasibility of this approach. To simulate a real complex condition, human serum was used to demonstrate its practicability in real world applications. Matrix-assisted laser desorption/ionization mass spectrometry (MALDI-MS) was used to confirm the sensing results.

Experimental section

Reagents and materials Acetonitrile, 2,5-dihydroxybenzoic acid (DHB), α-casein (from bovine milk), bradykinin, insulin, and trypsin (from bovine pancreas, TPCK treated) were obtained from Sigma (St. Louis, MO). Acetonitrile, hydrochloric acid, and trifluoroacetic acid (TFA) were obtained from Merck (Darmstadt, Germany). Ammonium hydrogencarbonate, hydrogen peroxide (35%), phosphoric acid (85%), trisodium citrate (99.5%), and sulfuric acid were purchased from Riedel-de Häen (Seelze, Germany). Ethanol and hydrogen tetrachloroaurate(III) tetrahydrate ($HAuCl_4$) was obtained from Showa (Tokyo, Japan). Melittin, nitric acid (65%), and tetraethoxysilane (TEOS, 99%) were purchased from Fluka (Steinheim, Germany). Methanol was obtained from Tedia (Fairfield, OH). *N*-[3-(trimethoxysilyl)propyl]-ethylenediamine (EDAS, 80%) and titanium (IV) isopropoxide (97%) were purchased from Aldrich (Steinheim, Germany). Cover glass slides (18 mm × 18 mm × 0.15 mm) were purchased from Matsunami Glass (Osaka, Japan). Human serum was donated by healthy individuals.

Preparation of Au NPs All glassware and stirring bars were rinsed with a solution of HNO_3/HCl (1/3, *v*/*v*) and deionized water. Au NPs were generated based on the Frens method with trisodium citrate as the reducing agent [11]. Different sizes of Au NPs were generated by adjusting the relative amount of $HAuCl_4$ and trisodium citrate. Au NPs with particle size of ca. 84 nm were generated by heating up an aqueous tetrachloroaurate solution (0.1 mg/mL, 100 mL) in a 100-mL glass vial to boiling point. Trisodium citrate (1%, 1.0 mL) was added while stirring, and color change was observed. The solution turned from pale yellow to dark purple, and then to deep red, at which point monodisperse spherical particles were formed. The solution was continuously heated while stirring for an additional 5 min. After cooling to room temperature, the suspension of Au NPs was centrifuged at 2,500 rpm for 10 min. The supernatant (99.5 mL) was removed by a pipette. The concentration of the NP suspension was estimated by measuring the optical density (OD) at a wavelength of 540 nm ($OD_{540\ nm}$). Because the $OD_{540\ nm}$ of the original NP suspension exceeded 1, a diluted NP suspension was prepared by mixing the remaining NP suspension (0.1 mL) with deionized water (0.9 mL) prior OD measurement. Based on this, the original OD was then calculated by multiplying the detected OD value with the diluting factor (i.e., 10). The $OD_{540\ nm}$ of the original remaining NP suspension was adjusted to 8 by mixing with deionized water before using the NP suspension for the fabrication of the LSPR glass slides. The particle size of the generated Au NPs was 83.8±13.3 nm.

Au NPs with the particle sizes of ca. 20 nm and ca. 66 nm were generated by mixing aqueous $HAuCl_4$ (0.1 mg/mL, 50 mL) with 1 mL and 0.4 mL of aqueous trisodium citrate (1%), respectively. Au NPs (18.9±2.0 nm) were readily used for LSPR fabrication after the reaction. However, Au NP (66±8.5 nm) needed to be filtered to remove smaller NPs by centrifugation of the suspension at a speed of 4,000 rpm for 10 min. After removing the supernatant, the remaining Au NPs were then diluted to 15 mL with deionized water. The NP suspension was stored 4 °C before use.

Fabrication of LSPR glass slides Glass slides were pretreated by soaking in a piranha solution [H_2SO_4/H_2O_2, 3: 1 (*v*/*v*)] for 30 min to remove impurities, followed by washing them with water and methanol under sonication. Glass slides were placed in methanol before use, and then dried by a hairdryer before surface modification. The

piranha solution is highly reactive, and thus, should be handled with care. Initially, the surface of the glass slide was modified with a thin film of EDAS by depositing 0.5 mL of EDAS (0.25%, *v*/*v*) prepared in deionized water for 10 min. The slide was rinsed with deionized water to remove unbound EDAS, dried with a hairdryer, and heated in an oven at 120 °C for 1 h to eliminate the remaining water and to strengthen EDAS binding. After cooling to room temperature, the glass slide was put in a Petri dish and deposited with the Au NP suspension (0.1 mL), as prepared above. A water droplet (diameter, ca. 11 mm) was then formed on the glass slide due to surface tension. The Petri dish was covered to reduce possibilities of water evaporation. Au NPs were expected to attach to the slide surface via electrostatic interactions. After standing at ambient temperature for 4 h, the slide was rinsed with deionized water to remove unbound Au NPs and dried using a hairdryer. A TEOS solution consisting of TEOS (4.5 mL), deionized water (1 mL), and hydrochloric acid (0.1 M, 0.5 mL) was prepared under stirring with a stirring speed of 700 rpm for 4 h. The generated TEOS solution was diluted 10^4-fold with deionized water. The slide, as prepared above, was spin-coated with the diluted TEOS solution (100 μL) in two steps: at 1,000 rpm for 15 s and then at 1,300 rpm for 10 s. After spin-coating, the resultant glass slide was deposited with 0.5 mL aqueous EDAS (0.25%, *v*/*v*) and allowed to stand at ambient condition for 10 min, followed by rinsing with deionized water to remove excess EDAS. After drying by a hairdryer, the glass slide was placed in an oven set at 120 °C for 1 h to further strengthen the silane binding. After cooling to room temperature, the glass slide was transferred on a Petri dish, deposited with Au NP suspension (0.1 mL), covered with dish cover, and incubated at ambient condition for 4 h. After rinsing with deionized water, the resultant glass slide was dried with a hairdryer.

Titania sol (0.3 mg/mL) was prepared by dissolving titanium (IV) isopropoxide (0.5 mL) in ethanol. The glass slide obtained above was then spin-coated with the titania sol (100 μL) in two steps: at 1,000 rpm for 15 s and then at 1,300 rpm for 10 s. After drying, the glass slide TiO_2-Glass@Au NPs was ready for use in the LSPR experiment.

LSPR and MALDI-MS analysis The tryptic digestion product of α-casein was initially used as sample. The digest solution was prepared by incubating aqueous α-casein (10^{-4} M, 1.5 mL) with trypsin (2 mg/mL, 40 μL) prepared in ammonium hydrogencarbonate (50 mM, pH 8) at 37 °C for 18 h. The tryptic digestion product was then diluted with TFA (0.15%) to a given concentration before LSPR analysis. Similarly, serum samples were prepared by diluting with aqueous TFA (0.15%) prior analysis. When performing LSPR analysis, the sample (0.1 mL) was deposited on the TiO_2-Glass@Au NPs, followed by vigorously mixing by pipetting on the glass slide at about 1 min to accelerate the selective-trapping of target species by the substrate. Subsequently, a solution of TFA(0.15%)/acetonitrile (1:1, *v*/*v*; 1 mL × 3) was used to rinse the surface of the glass slide to remove unbound species. The slide was then dried with nitrogen gas. Consequently, the slide was prepared for LSPR spectroscopic analysis. For further confirmation of the results, MALDI-MS analysis was performed. The glass slide was adhered on a MALDI sample target, followed by deposition of aqueous 2,5-DHB solution (40 mg/mL, 0.4 μL) consisting of 1% phosphoric acid. After solvent evaporation, the sample was ready for MALDI-MS analysis.

Instrumentation All LSPR analyses were performed by a Varian Cary 50 absorption spectrofluorophotometer (Melbourne, Australia). MALDI-MS analyses were carried out by a Biflex III MALDI-time of flight mass spectrometer (Bruker Daltonics, Germany). Scanning electron microscopy (SEM) was conducted using a JEOL JSM-7401 F instrument (Tokyo, Japan).

Results and discussion

In order to generate LSPR-sensing substrates with absorption bands in the NIR, self-assembled Au NPs were generated on a glass slide. Different sizes of Au NPs were used for the fabrication of the LSPR glass slides. Figure 1 displays the LSPR spectra of LBL Au NPs on glass slides. The bottom spectrum was obtained by immobilizing LBL Au NPs (ca. 20 nm) on the glass slide. Apparently, the maximum absorption band only reveals at wavelength of ~600 nm. Larger Au NPs (ca. 66 nm) were used for fabrication of the LSPR glass slides with LBL Au NPs. The maximum absorption band appears at wavelength, ca. 660 nm (the central spectrum in Fig. 1). When LBL Au NPs (ca. 84 nm) were immobilized on the glass slide, the maximum absorption band appears in the NIR (ca. 800 nm; the spectrum on the top in Fig. 1). These LSPR glass slides were then used as sensing substrates for the LSPR analysis in this study.

The photograph of the slide coated with the first layer of Au NPs (ca. 84 nm), which shows a red circle formed on the slide, is shown in Fig. 2a. After immobilizing the second layer of Au NPs (ca. 84 nm) on the slide (Fig. 2b), the Au NP layers seemed to appear as dark purple. Figure 2c, d present the corresponding SEM images of the glass slide coated with self-assembling Au NPs once and twice, respectively. Incidentally, the density of Au NPs on the glass slide was increased after the two-layer deposition.

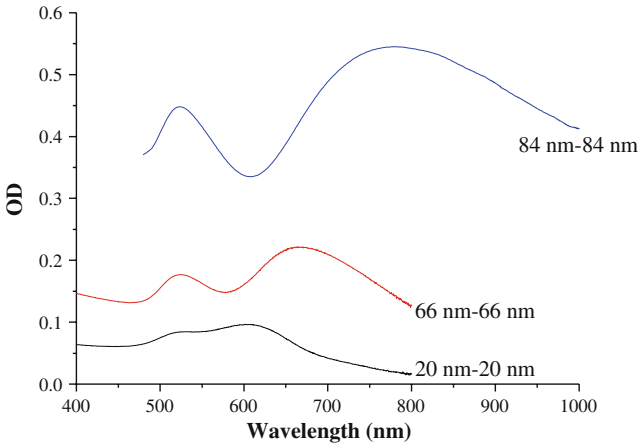

Fig. 1 LSPR absorption spectra of the glass slides immobilized with two layers of Au NPs. The particle sizes of the Au NPs were ca. 20 nm, ca. 66 nm, and ca. 84 nm (*from bottom to top*)

The coverage of the first layer of Au NPs on the slide is ca. 37.1%, while it increased to 53.4% after two layers of Au NP deposition in terms of the relative ratio of the surface area of the Au NPs occupied on the surface area of the glass slide. Figure 2e, f present the corresponding SEM images of the cross-section of the slides immobilized with one and two layers of Au NPs, respectively.

Because all the sensing experiments were conducted by using 0.15% TFA as the solvent, we initially examined whether depositing the solvent alone on the sensing substrate might cause any LSPR shift. Figure 3 displays the LSPR spectra obtained by using Au NPs (ca. 84 nm) for fabrication of the LSPR-sensing substrate: Glass@Au NPs alone (I), LSPR absorption spectra of the TiO_2-Glass@Au NPs obtained before (II) and after (III) deposition of 0.15% TFA (0.1 mL) as a blank control examination. There is a red shift arising from band I to band II because of the coating of TiO_2. However, there is no shift observed between the bands II and III. The results demonstrate that

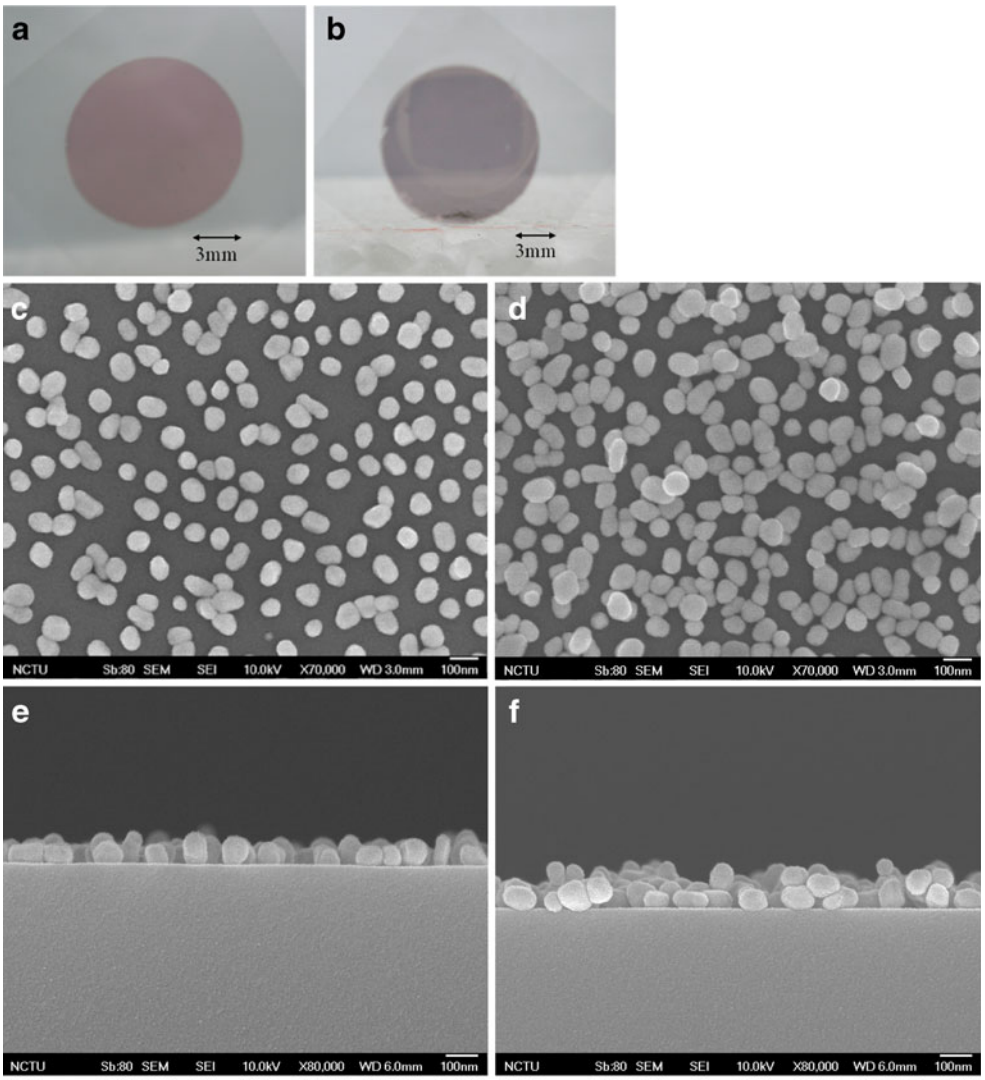

Fig. 2 Photographs of the glass slide immobilized **a** with one layer of Au NPs (ca. 84 nm) and **b** with two layers of Au NPs (ca. 84 nm). SEM images of the glass slide immobilized with **c** one layer of Au NPs (ca. 84 nm) and **d** two layers of Au NPs (ca. 84 nm). The corresponding SEM images **e** and **f** of the cross section of the slides for obtaining panels *c* and *d*, respectively

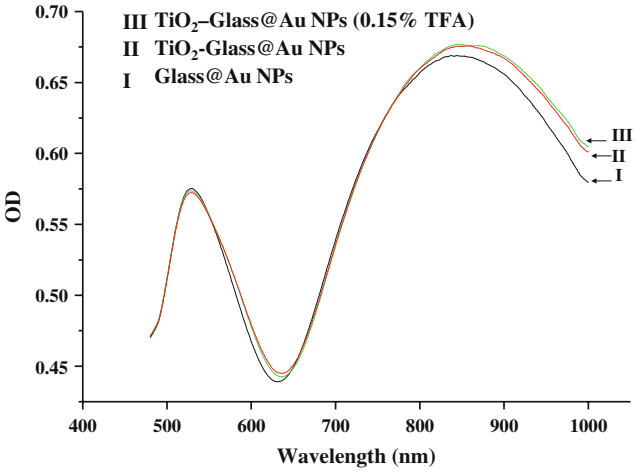

Fig. 3 LSPR absorption spectra obtained by using Au NPs (ca. 84 nm) for fabrication of the LSPR-sensing substrate: Glass@Au NPs alone (*I*), LSPR absorption spectra of the TiO_2-Glass@Au NPs obtained before (*II*) and after (*III*) deposition of 0.15% TFA (0.1 mL) as a blank control examination

the solvent does not cause any LSPR shift during sensing processes.

Next, a TiO_2-Glass@Au NPs/ca. 84 nm was used as the LSPR-sensing substrate for phosphopeptides. Tryptic digest of α-casein was used as the sample. Figure 4a displays the LSPR spectra of the Glass@Au NPs (band I) and the TiO_2-Glass@Au NPs before (band II) and after (band III), which interacted with the tryptic digest of α-casein (10^{-6} M, 0.1 mL). A red shift arising from 847 nm to 858 nm was evident after coating a thin layer of titania on the Glass@Au NPs. After interacting with the digest sample, the maximum absorption band was further shifted to 869 nm. For comparison, the results obtained from using smaller sizes of Au NPs (58.5±7.2 nm) were preformed. Figure 4b present the LSPR spectra of the Glass@Au NPs (band I) and the TiO_2-Glass@Au NPs (58.5±7.2 nm) before (band II) and after (band III) interacting with the same sample used to obtain the absorption band III in Fig. 4a. There was a red shift arising from the absorption band at 684 nm to 690 nm after the TiO_2-Glass@Au NPs sensed the sample. The red shift occurring at the LSPR absorption band was only half of that obtained in Fig. 4a. Results confirm that there was a larger shift that occurred when the initial LSPR absorption band of the glass slide appeared in the NIR than when it appeared in the visible region. Additionally, the sensing steps were conducted by pipetting the sample solution directly on the chip for 1 min to accelerate the selective-trapping of target species because we found the shift arising from the binding was similar to that obtained for standing the sample on the chip for 1 h. To shorten the analysis time, vigorous mixing by pipetting on the sensing chip for 1 min was used in this work.

To further validate the results obtained in Fig. 4a, MALDI-MS was used to analyze the species trapped on

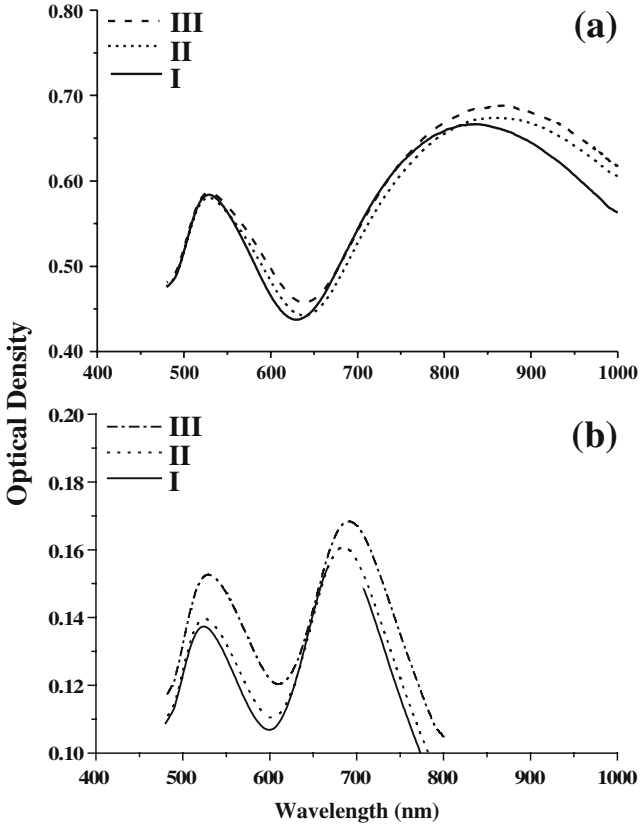

Fig. 4 **a** LSPR absorption spectra obtained by using Au NPs (ca. 84 nm) for fabrication of the LSPR-sensing substrate: Glass@Au NPs alone (*I*), LSPR absorption spectra of the TiO_2-Glass@Au NPs obtained before (*II*) and after (*III*) deposition of the tryptic digest of α-casein (10^{-6} M, 0.1 mL). **b** LSPR absorption spectra obtained by using Au NPs (58.5±7.2 nm) for fabrication of the LSPR-sensing substrate: Glass@Au NPs alone (*I*), LSPR absorption spectra of the TiO_2-Glass@Au NPs obtained before (*II*) and after (*III*) deposition of the tryptic digest of α-casein (10^{-6} M, 0.1 mL)

the TiO_2-Glass@Au NPs. Figure 5a displays the MALDI mass spectrum of the same glass slide used for obtaining the absorption band III in Fig. 4a, while Fig. 5b presents the direct MALDI mass spectrum of the tryptic digest of α-casein (10^{-6} M). In Fig. 5a, the peaks at *m/z* 1,661.1; 1,943.7; 1,952.0; 2,634.9; 2,720.9; 2,736.9; 3,008.0; and 3,088.0 (marked with asterisks) were attributed to phosphopeptides (see Table 1). The peak at *m/z* 2,637.8 is presumably from the phosphopeptide peak at *m/z* 2,720.9 with the loss of a HPO_3^-. All peaks were derived from phosphopeptides in Fig. 5a. However, in Fig. 5b, there is only one peak at *m/z* 1951.7 derived from phosphopeptide (S2/#152–167). The results indicate that the TiO_2-Glass@Au NPs can selectively trap phosphopeptides from complex tryptic digestion samples, while the red shift observed in Fig. 4a is due to the binding of phosphopeptides on the LSPR glass slide.

Additionally, the relationship between the sample concentration and LSPR responses was examined. Figure 6

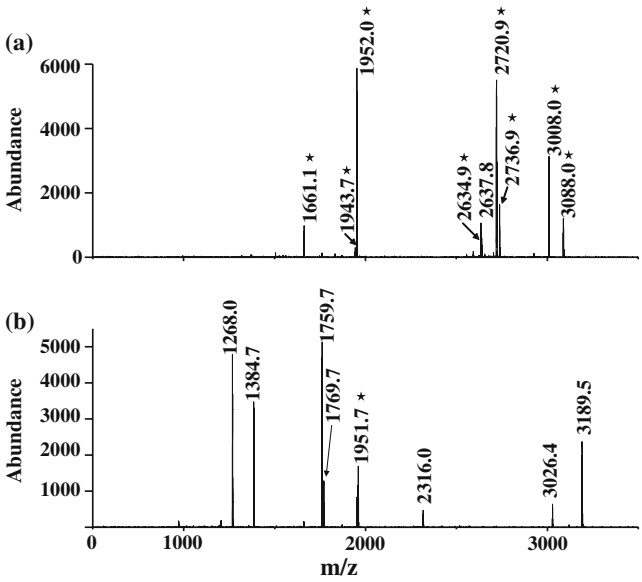

Fig. 5 **a** MALDI mass spectrum of the sensing substrate used to obtain plot III in Fig. 4a. 2,5-DHB (40 mg/mL, 0.4 μL) containing 1% phosphoric acid was applied on the substrate prior to MALDI-MS analysis. **b** Direct MALDI mass spectrum of the tryptic digest of α-casein (10^{-6} M). Phosphopeptide peaks were marked with *asterisks*

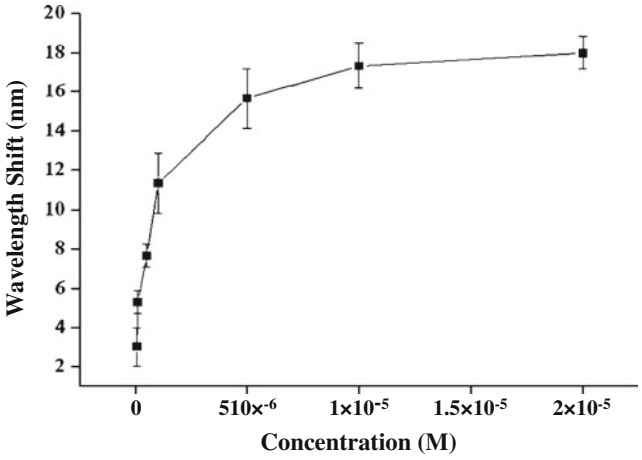

Fig. 6 Plot of the LSPR wavelength shift of the tryptic digest product of α-casein as a function of its concentration. The TiO_2-GlassAu NPs (ca. 84 nm) glass slide was used as the sensing chip

presents the curve plotted from the wavelength shift of the maximum LSPR absorption band before and after depositing the sample, (i.e., tryptic digest of α-casein) on the LSPR TiO_2-Glass@Au NPs sensing slide as a function of the sample concentration. There was only a slight red shift of the LSPR absorption band as the concentration of the tryptic digestion product of α-casein increased to beyond 10^{-5} M, indicating that the sensing slide was saturated as the concentration $>10^{-5}$ M owing to the saturation by the binding of phosphopeptides. Furthermore, the detection limit was ca. 5 pmol (50 nM, 0.1 mL) at the wavelength shift of 3 nm. The results were better than by using one layer of Au NPs alone for the LSPR TiO_2-Glass@Au NPs glass slide as the sensing substrate [1]. In the previous study, the detection limit was ca. 25 pmol with a wavelength shift of only 1 nm. Additionally, the maxima shift of the absorption band in the NIR region is as large as 18 nm, while it is only 7 nm while using one layer of Au NPs alone for the LSPR TiO_2-Glass@Au NPs glass slide as the sensing substrate. That is, the current approach truly makes improvement for sensing phosphopeptides in terms of sensitivity. Additionally, it is required to use well control sized Au NPs for fabricating the sensing chip and to coat the as-prepared Au NPs on the chip as suggested in the experimental section. Therefore, reproducible LSPR absorption spectra can be obtained, which is important to ensure the reproducible results. On the basis of the error bar of the plot shown in Fig. 6, the reproducibility of this approach is desirable while our suggested experimental conditions were conducted for the sensing experiments.

To simulate this LSPR approach in real world applications, human serum was used as sample. Serum samples are complex and contain abundant proteins and metabolites. We previously demonstrated that titania and alumina-coated iron oxide magnetic NPs (Fe_3O_4@TiO_2 and Fe_3O_4@Al_2O_3 MNPs) can be used as affinity probes to selectively trap phosphorylated fibrinopeptide A from complex serum samples [23]. Fibrinopeptide A is derived from the thrombin digestion of fibrinogen, which plays a significant role in vertebrate blood clotting. Its concentration in blood plasma ranges from 4.4 to 11.7 μM [24]. About 20–30% of

Table 1 Peaks observed in Fig. 4a

Observed $[M+H]^+$	Theoretical $[M+H]^+$	Sequences
1,661.1	1,660.8	VPQLEIVPNsAEER (S1/106–119)
1,943.7	1,943.7	DIGsEsTEDQAMEDIK (S1/43–58)
1,952.0	1,951.9	KTVDMEsTEVFTKKTK (S2/152–167)
2,634.9	2,634.9	NTMEHVsssEESIIsQETYK (S2/2–21)
2,720.9	2,721.0	QMEAEsIsssEEIVPNsVEQK (S1/59–79)
2,736.9	2,737.0	QMEAEsIsssEEIVPNsVEQK (S1/59–79)
3,008.0	3,008.0	NANEEEYSIGsssEEsAEVATEEVK (S2/46–70)
3,088.0	3,087.3	sTsEENSKKTVDMEsTEVFTKKTL (S2/129–153)

s phosphorylated serine, *M* oxidized methionine

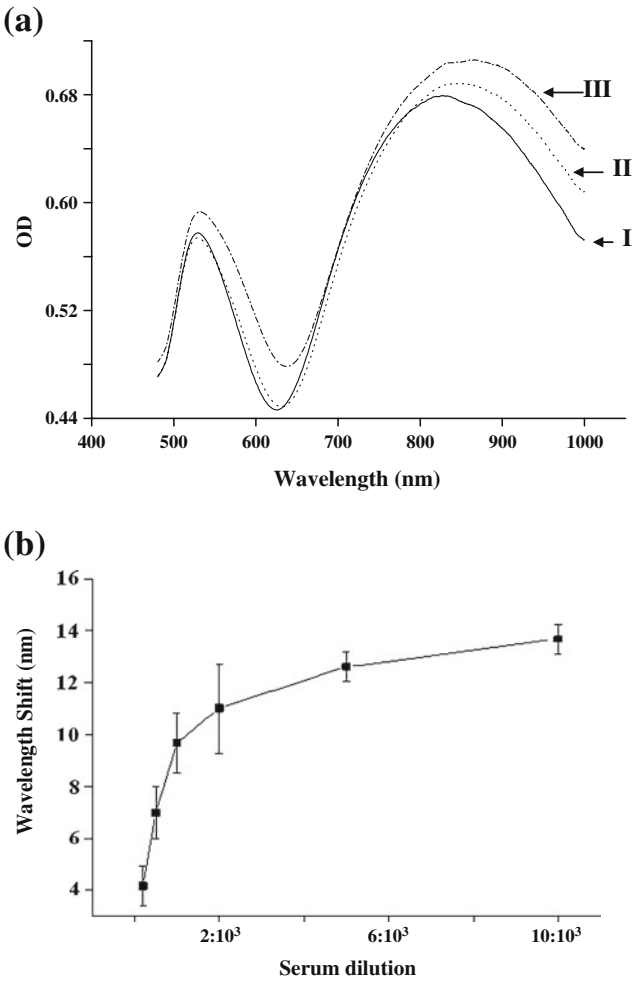

Fig. 7 **a** LSPR absorption spectra of Glass@Au NPs (ca. 84 nm) alone (*I*) and the TiO_2-GlassAu NPs (ca. 84 nm) obtained before (*II*) and after (*III*) depositing of 100-fold diluted serum sample **b** Plot of the LSPR wavelength shift of the serum sample as a function of dilution

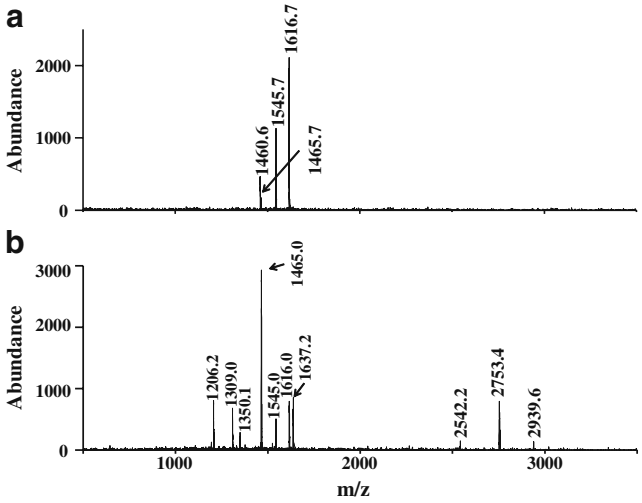

Fig. 8 **a** MALDI mass spectrum of the sensing substrate used to obtain plot III in Fig. 7a. **b** Direct MALDI mass spectrum of the 100-fold diluted serum sample. 2,5-DHB (40 mg/mL, 0.4 μL) containing 1% phosphoric acid was applied on the substrate before MALDI-MS analysis

fibrinopeptide A forms phosphorylated fibrinopeptide A after thrombin digestion [23,25]. Figure 7a presents the LSPR spectra of Glass@Au NPs (plot I) and TiO_2-Glass@Au NPs before (band II) and after (band III) sensing a serum sample diluted 100-fold by 0.15% TFA. The maximum LSPR absorption band shifted from 854 to 865 nm after depositing the serum sample. To examine the quantitative capability of this approach, the serum sample was prepared by series dilution of 100–5,000-fold with 0.15%TFA. Figure 7b presents the curve plotted with the LSPR wavelength shift obtained before and after depositing the serum sample versus the concentration of the serum sample. The wavelength shift was proportional to the concentration of the serum samples. MALDI-MS was used for the characterization of the species trapped by the LSPR glass slide. Figure 8a presents the MALDI mass spectrum obtained from the same slide used for obtaining plot III in Fig. 7a. The peaks at *m*/*z* 1,460.6; 1,545.7; and 1,616.7 derived from phosphorylated fibrinopeptide A appeared in the mass spectrum. The peak at *m*/*z* 1,465.7 is the fragment of the peak at *m*/*z* 1,545.7 with a loss of a HPO_3^-. Table 2 lists the detailed sequences of these peaks. Figure 8b displays the direct MALDI mass spectrum of the same serum sample used to obtain the result in Fig. 8a. Numerous peaks appeared in the mass spectrum. Results indicate that the LSPR-sensing substrate could selectively trap phosphorylated fibrinopeptide A species from complex serum samples. The LSPR-sensing approach combined with MALDI-MS analysis can simultaneously provide quantitative and qualitative analysis. Lately, it has been noted that the level of fibrinopeptide A in serum may be higher in the sera of cancer patients [26,27]. Thus, it is meaningful for this LSPR approach to be used in quick examinations of the level of phosphorylated fibrinopeptide A in human serum. In addition, although all the samples above containing phosphor-serine peptides, this approach is also suitable for being used to detect phospho-threonine and -tyrosine peptides. The LSPR TiO_2-Glass@Au NPs chip recognizes phosphopeptides mainly through Ti–phosphate interactions.

Table 2 Peaks observed in Fig. 8

Observed $[M+H]^+$	Theoretical $[M+H]^+$	Sequences	Identification
1,460.6	1,460.6	ADsGEGDFLAEGGGV	Fibrinopeptide A (1–15)
1,545.7	1,545.6	DsGEGDFLAEGGGVR	Fibrinopeptide A (2–16)
1,616.7	1,616.7	ADsGEGDFLAEGGGVR	Fibrinopeptide A (1–16)

s phosphorylated serine

Conclusions

We have demonstrated that TiO_2-Glass@Au NPs with the LSPR absorption band in the NIR of electromagnetic spectrum can be used to selectively sense phosphopeptides from complex samples, including tryptic digest samples and serum samples. This current approach can be used to detect as low as 5 pmol of phosphopeptides in a sample. The sensitivity is much better than that obtained from using one layer of Au NPs alone for the LSPR TiO_2-Glass@Au NPs sensing substrate. Furthermore, the shift of the maximum absorption band in the NIR region is much larger than that obtained from one layer Au NPs of LSPR TiO_2-Glass@Au NPs sensing chip for an equal concentration of phosphopeptides. By combining this LSPR approach with MALDI-MS analysis, the level of phosphorylated peptides can be quantitatively and qualitatively determined. On the basis of the results demonstrated in this study, it is possible to employ this LSPR approach in rapidly determining the level of phosphorylated fibrinopeptide A in serum samples. Owing to such advantage, including its short analysis time, speed, and low cost, this approach can be used for potential cancer diagnosis, especially when screening the level of phosphorylated fibrinopeptide A in human serum.

Acknowledgments We thank the National Science Council of Taiwan for supporting this work financially. We also thank Dr. Wei-Yu Chen and Ms. Tsai-Jung Yu for their assistance in obtaining the SEM images, and Mr. Kai-Wei Han for his assistance in preparing the figures.

References

1. Kuong C-L, Chen W-Y, Chen Y-C (2007) Anal Bioanal Chem 387:2091–2099
2. Okamoto T, Yamaguchi I, Kobayashi T (2000) Opt Lett 25:372–374
3. Nath N, Chilkoti A (2002) Anal Chem 74:504–509
4. Nath N, Chilkoti A (2004) Anal Chem 76:5370–5378
5. Nath N, Chilkoti A (2004) J Fluoresc 14:377–389
6. Lin H-Y, Chen C-T, Chen Y-C (2006) Anal Chem 78:6873–6878
7. Haes AJ, Van Duyne RP (2002) J Am Chem Soc 124:10596–10604
8. Wang Y, Qian W, Tan Y, Ding S (2008) Biosens Bioelectron 23:1166–1170
9. Mayer KM, Lee S, Liao H, Rostro BC, Fuentes A, Scully PT, Nehl CL, Hafner JH (2008) ACS Nano 2:687–692
10. Lee S, Kathryn M, Mayer KM, Hafner JH (2009) Anal Chem 81:4450–4455
11. Frens G (1973) Nat Phys Sci 241:20–22
12. Schierhorn M, Kotov NA, Liz-Marzán LM (2002) Langmuir 18:3694–3697
13. Jiang C, Markutsya S, Tsukruk VV (2004) Langmuir 20:882–890
14. Lu C, Mohwald H, Fery A (2007) J Phys Chem C 111:10082–10087
15. Pinkse MWH, Uitto PM, Hilhorst MJ, Ooms B, Heck AJR (2004) Anal Chem 76:3935–3943
16. Liang S-S, Makamba H, Huang S-Y, Chen S-H (2006) J Chromatogr A 1116:38–45
17. Rinalducci S, Larsen MR, Mohammed S, Zolla L (2006) J Proteome Res 5:973–982
18. Larsen MR, Thingholm TE, Jensen ON, Roepstorff P, Jorgensen TJD (2005) Mol Cell Proteomics 4:873–886
19. Sano A, Nakamura H (2004) Anal Sci 20:565–566
20. Kweon HK, Hakansson K (2008) J Proteome Res 7:749–755
21. Chen C-T, Chen Y-C (2008) J Biomed Nanotechnol 4:73–79
22. Chen C-T, Chen Y-C (2005) Anal Chem 77:5912–5919
23. Hettasch JM, Strickland E, Lord ST (1993) Biochemistry 32:107–113
24. Selmeci L, Székely M, Soos P, Seres L, Klinga N, Geiger A, Acsady G (2006) Free Radic Res 40:952–958
25. Maurer MC, Trosset J-Y, Lester CC, DiBella EE, Scheraga HA (1998) Biochemistry 37:5888–5902
26. Ebert MP, Niemeyer D, Deininger SO, Wex T, Knippig C, Hoffmann J, Sauer J, Albrecht W, Malfertheiner P, Röcken C (2006) J Proteome Res 5:2152–2158
27. Ogata Y, Hepplmann CJ, Charlesworth MC, Madden BJ, Miller MN, Kalli KR, Cilby WA, Bergen HR III, Saggese DA, Muddiman DC (2006) J Proteome Res 5:3318–3325